

6th International Workshop on Heavy Quarkonium
Dec. 4, 2008, Nara Women's University, Japan

Next-To-Leading-Order QCD Corrections to J/ψ Production at Hadron Colliders

Jian-Xiong Wang

Institute of High Energy Physics,
Chinese Academy of Science

In collaboration with Bin Gong, Xue. Qian Li



Contents

- ➊ Introduction
- ➋ NLO QCD corrections to J/ψ polarization via S-wave color singlet state
- ➌ NLO QCD corrections to J/ψ production via S-wave color octet states $(^1S_0^{(8)}, ^3S_1^{(8)})$
- ➍ NLO QCD corrections to $J/\psi + gg$ at B-factory
- ➎ Summary and conclusion

1. Introduction

QCD, Hadronization, NRQCD, Color-singlet, Color-Octet
C quark heavy, clear signal to detect J/ψ

P_t distribution of J/ψ production at Tevatron

P_t distribution of J/ψ polarization at Tevatron

J/ψ production at B factories

J/ψ production at DESY ep collider HERA

J/ψ production at Fix Target Experiments

Next To Leading Order QCD Corrections
are very large.

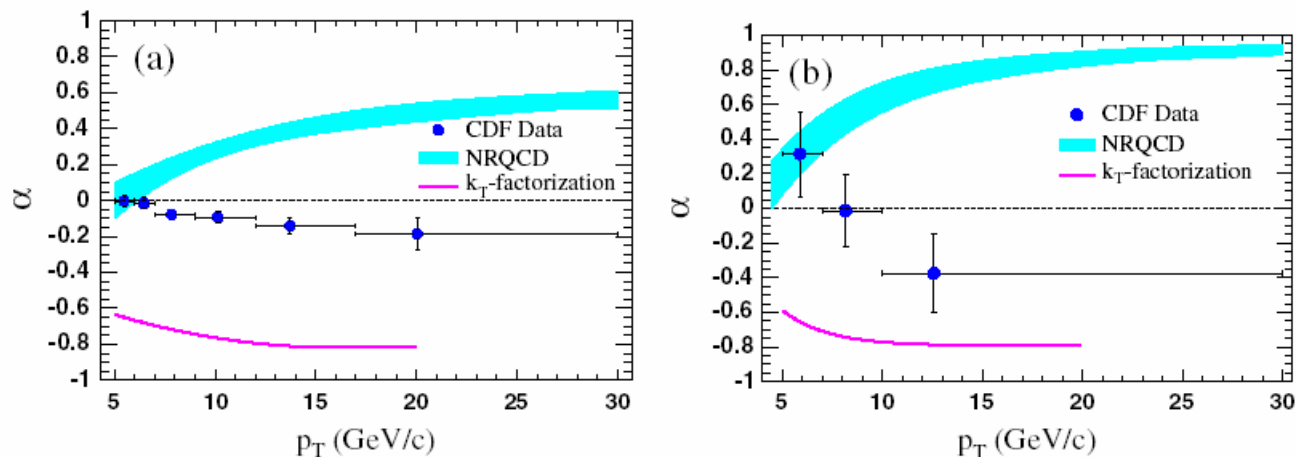
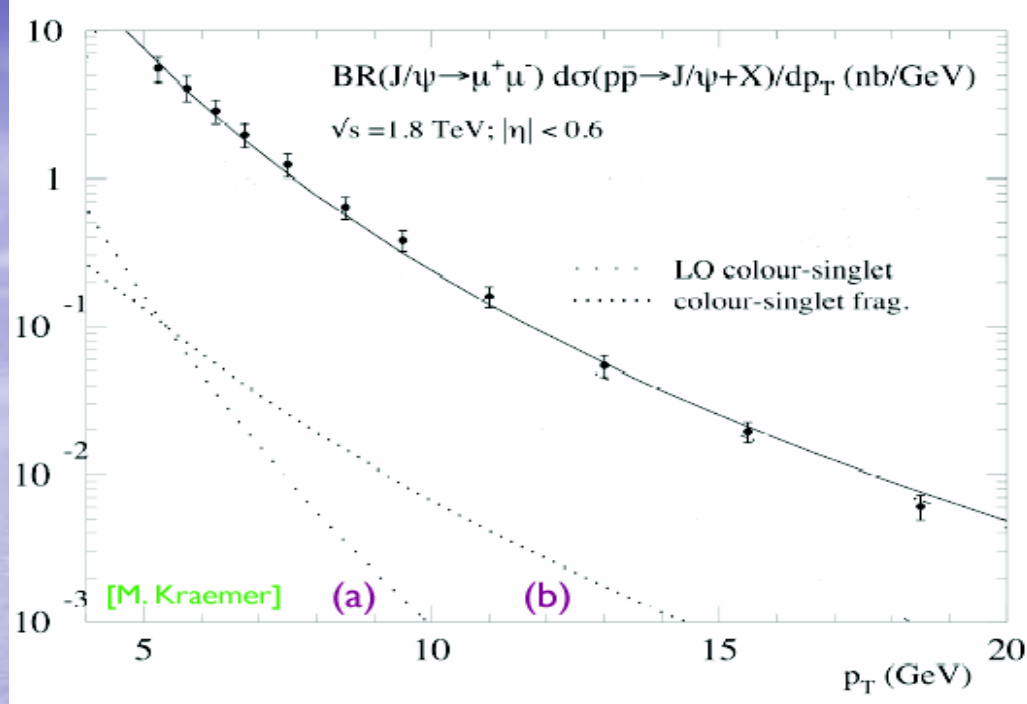


FIG. 4 (color online). Prompt polarizations as functions of p_T : (a) J/ψ and (b) $\psi(2S)$. The band (line) is the prediction from NRQCD [4] (the k_T -factorization model [9]).

- Recently NLO QCD corrections to J/ψ hadron production have been calculated and the results show that the total cross section is boosted by a factor of about 2 while the J/ψ transverse momentum p_t distribution is enhanced more and more as p_t becomes larger.

J. Campbell, F. Maltoni and F. Tramontano, Phys. Rev. Lett. **98**, 252002 (2007)

- Real correction process $gg \rightarrow J/\psi c\bar{c}$ was calculated. It gives sizable contribution to p_t distribution of J/ψ at high p_t region, and it alone gives almost **unpolarized** result.

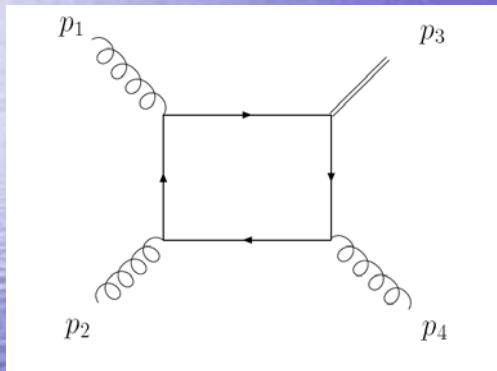
P. Artoisenet, J. P. Lansberg and F. Maltoni, Phys. Lett. **B653**, 60 (2007).

C. F. Qiao and J. X. Wang, Phys. Rev. **D69**, 014015 (2004).



So how about the J/ψ polarization status when NLO QCD corrections are included?

NLO QCD corrections to J/ψ polarization via S-wave color singlet state



$$\frac{d\hat{\sigma}^B}{d\hat{t}} = \frac{5\pi\alpha_s^3 |R_s(0)|^2 [\hat{s}^2(\hat{s}-1)^2 + \hat{t}^2(\hat{t}-1)^2 + \hat{u}^2(\hat{u}-1)^2]}{144m_c^5 \hat{s}^2(\hat{s}-1)^2(\hat{t}-1)^2(\hat{u}-1)^2}$$

$$\sigma^B = \int dx_1 dx_2 G_g(x_1, \mu_f) G_g(x_2, \mu_f) \hat{\sigma}^B$$

$$\hat{s} = \frac{(p_1+p_2)^2}{4m_c^2} \quad \hat{t} = \frac{(p_1-p_3)^2}{4m_c^2} \quad \hat{u} = \frac{(p_1-p_4)^2}{4m_c^2}$$

LO Cross Section

VIRTUAL CORRECTIONS

$$\frac{d\hat{\sigma}^V}{dt} \propto 2\text{Re}(M^B M^{V*})$$

$$\sigma^V = \int dx_1 dx_2 G_g(x_1, \mu_f) G_g(x_2, \mu_f) \hat{\sigma}^V$$

M^V is UV and Coulomb finite, but still contains the IR divergences:

$$M^V|_{IR} = \left[\frac{\alpha_s}{2\pi} \frac{\Gamma(1-\epsilon)}{\Gamma(1-2\epsilon)} \left(\frac{4\pi\mu_r^2}{s_{12}} \right)^\epsilon \right] \left(\frac{A_2^V}{\epsilon^2} + \frac{A_1^V}{\epsilon} \right) M^B$$

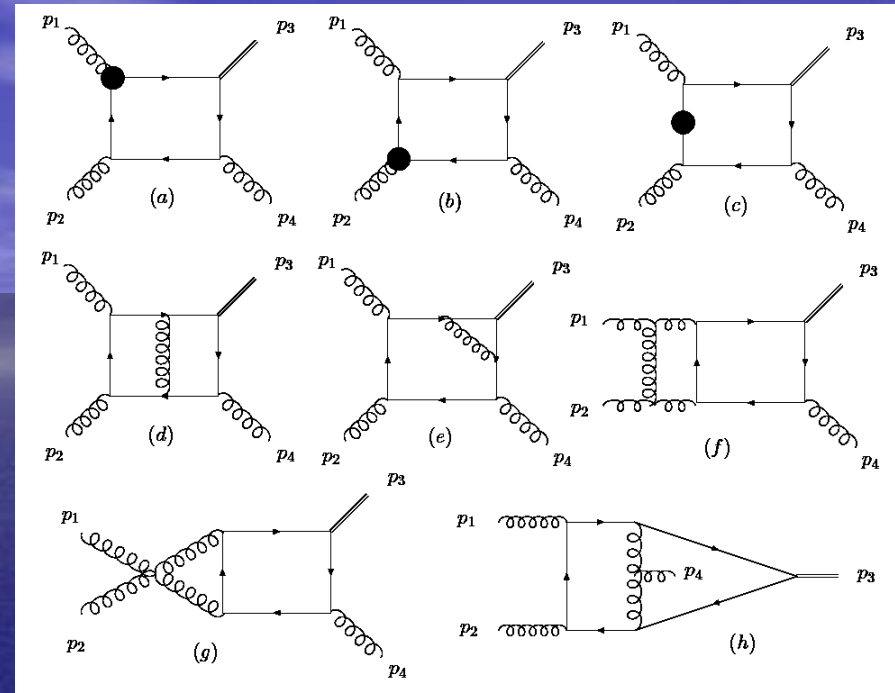
$$A_2^V = -\frac{9}{2} \quad A_1^V = -\frac{3}{2} \left[\ln\left(\frac{\hat{s}}{-\hat{t}}\right) + \ln\left(\frac{\hat{s}}{-\hat{u}}\right) \right] + \frac{1}{2} n_f - \frac{33}{4}$$

$$\delta Z_m^{OS} = -3C_F \frac{\alpha_s}{4\pi} \left[\frac{1}{\epsilon_{UV}} - \gamma_E + \ln \frac{4\pi\mu_r^2}{m_c^2} + \frac{4}{3} \right]$$

$$\delta Z_2^{OS} = -C_F \frac{\alpha_s}{4\pi} \left[\frac{1}{\epsilon_{UV}} + \frac{2}{\epsilon_{IR}} - 3\gamma_E + 3 \ln \frac{4\pi\mu_r^2}{m_c^2} + 4 \right]$$

$$\delta Z_3^{OS} = \frac{\alpha_s}{4\pi} \left[(\beta_0 - 2C_A) \left(\frac{1}{\epsilon_{UV}} - \frac{1}{\epsilon_{IR}} \right) \right]$$

$$\delta Z_g^{\overline{\text{MS}}} = -\frac{\beta_0}{2} \frac{\alpha_s}{4\pi} \left[\frac{1}{\epsilon_{UV}} - \gamma_E + \ln(4\pi) \right]$$



129 diagrams in total

only light quarks
are included in the
renormalization of
gluon field and
QCD gauge
coupling constant



$$g(p_1) + g(p_2) \rightarrow J/\psi(p_3) + g(p_4) + g(p_5) \quad (a)$$

$$g(p_1) + g(p_2) \rightarrow J/\psi(p_3) + q(p_4) + \bar{q}(p_5) \quad (b)$$

$$g(p_1) + q(p_2) \rightarrow J/\psi(p_3) + g(p_4) + q(p_5) \quad (c)$$

REAL CORRECTIONS

Two-cutoff phase space slicing method is applied

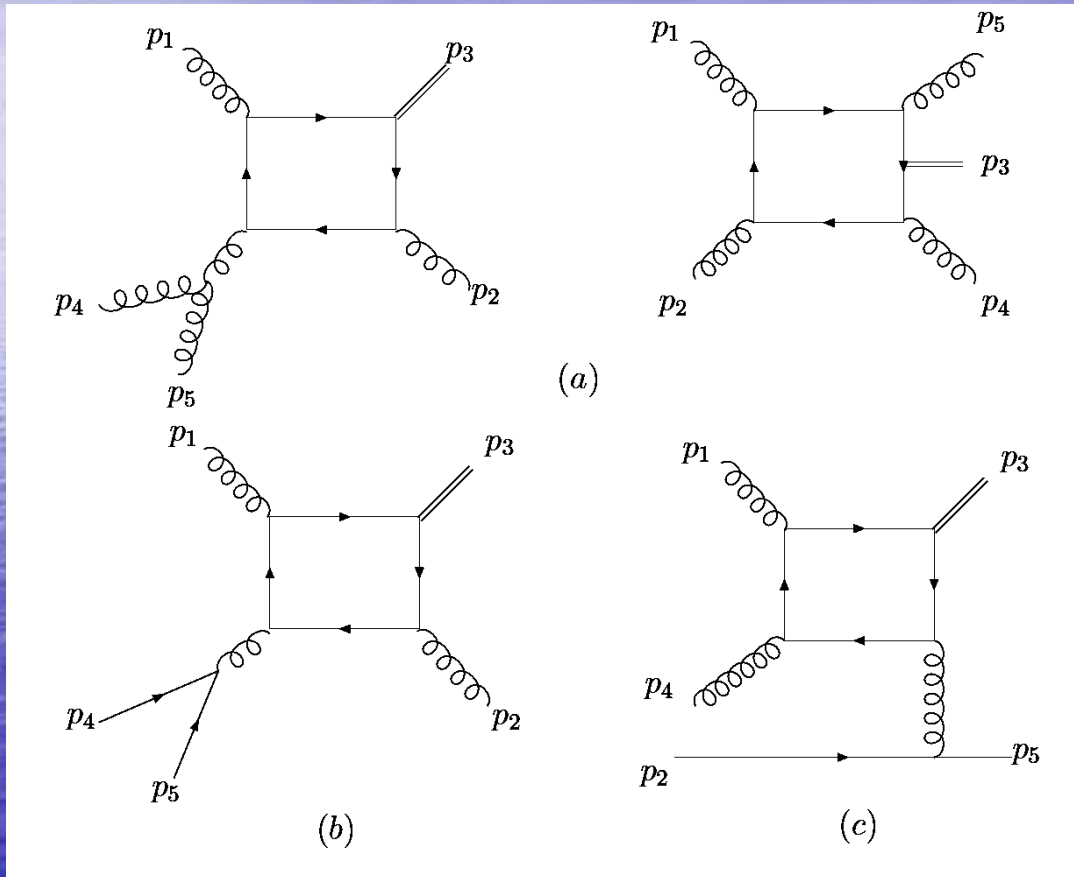
B. W. Harris and J. F. Owens, Phys. Rev. **D65**, 094032 (2002).

$$\sigma^R = \sigma^S + \sigma^{HC} + \sigma^{H\bar{C}}$$

☀ **Soft:** (a)

☀ **Final Collinear:**
(a) and (b)

☀ **Initial Collinear:**
(a) and (c)



Soft singularities caused by emitting soft gluons from the charm quark-antiquark pair in the s-wave color singlet J/ψ are canceled with each other. Only the process (a) where there could be a soft gluon emitted from the external gluons contains soft singularities.

SOFT

$$\hat{\sigma}^S = \hat{\sigma}^B \left[\frac{\alpha_s}{2\pi} \frac{\Gamma(1-\epsilon)}{\Gamma(1-2\epsilon)} \left(\frac{4\pi\mu_r^2}{s_{12}} \right)^\epsilon \right] \left(\frac{A_2^S}{\epsilon^2} + \frac{A_1^S}{\epsilon} + A_0^S \right)$$

$$A_2^S = 9$$

$$A_1^S = 3 \left[\ln \left(\frac{\hat{s} - 1}{-\hat{t}} \right) + \ln \left(\frac{\hat{s} - 1}{-\hat{u}} \right) \right] - 18 \ln \delta_s$$

$$\begin{aligned} A_0^S = & 18 \ln^2 \delta_s - 6 \ln \delta_s \left[\ln \left(\frac{\hat{s} - 1}{-\hat{t}} \right) + \ln \left(\frac{\hat{s} - 1}{-\hat{u}} \right) \right] \\ & + \frac{3}{2} \left[\ln^2 \left(\frac{\hat{s} - 1}{-\hat{t}} \right) + \ln^2 \left(\frac{\hat{s} - 1}{-\hat{u}} \right) \right] \\ & + 3 \left[\text{Li}_2 \left(\frac{-\hat{t}}{\hat{s} - 1} \right) + \text{Li}_2 \left(\frac{-\hat{u}}{\hat{s} - 1} \right) \right] \end{aligned}$$

$$\hat{\sigma}_f^{HC} = \hat{\sigma}^B \left[\frac{\alpha_s}{2\pi} \frac{\Gamma(1-\epsilon)}{\Gamma(1-2\epsilon)} \left(\frac{4\pi\mu_r^2}{s_{12}} \right)^\epsilon \right] \times \left(\frac{A_1^{g \rightarrow gg} + A_1^{g \rightarrow q\bar{q}}}{\epsilon} + A_0^{g \rightarrow gg} + A_0^{g \rightarrow q\bar{q}} \right)$$

$$\sigma_f^{HC} = \int dx_1 dx_2 G_g(x_1, \mu_f) G_g(x_2, \mu_f) \hat{\sigma}_f^{HC}$$

Final

$$A_1^{g \rightarrow gg} = 3(11/6 + 2 \ln \delta'_s)$$

$$A_0^{g \rightarrow gg} = 3 \left[67/18 - \pi^2/3 - \ln^2 \delta'_s - \ln \delta_c (11/6 + 2 \ln \delta'_s) \right]$$

$$A_1^{g \rightarrow q\bar{q}} = -n_f/3$$

$$A_0^{g \rightarrow q\bar{q}} = n_f/3 (\ln \delta_c - 5/3)$$

$$\delta'_s = \frac{s_{12}}{s_{12} + s_{45} - M_{J/\psi}^2} \simeq \frac{\hat{s}}{\hat{s} - 1} \delta_s$$

$$A_0^{sc} = A_1^{sc} \ln(s_{12}/\mu_f^2)$$

$$A_1^{sc}(g \rightarrow gg) = 6 \ln \delta_s + (33 - 2n_f)/6$$

**Hard
Collinear**

$$\sigma_i^{HC} = \sigma_{add}^{HC} + \int \hat{\sigma}_i^{HC} G_g(x_1, \mu_f) G_g(x_2, \mu_f) dx_1 dx_2$$

$$\sigma_{add}^{HC} \equiv \int \hat{\sigma}^B \left[\frac{\alpha_s}{2\pi} \frac{\Gamma(1-\epsilon)}{\Gamma(1-2\epsilon)} \left(\frac{4\pi\mu_r^2}{s_{12}} \right)^\epsilon \right] \times \left[G_g(x_1, \mu_f) \tilde{G}_g(x_2, \mu_f) + (x_1 \leftrightarrow x_2) \right] dx_1 dx_2$$

$$\hat{\sigma}_i^{HC} = 2\hat{\sigma}^B \left[\frac{\alpha_s}{2\pi} \frac{\Gamma(1-\epsilon)}{\Gamma(1-2\epsilon)} \left(\frac{4\pi\mu_r^2}{s_{12}} \right)^\epsilon \right] \times \left[\frac{A_1^{sc}(g \rightarrow gg)}{\epsilon} + A_0^{sc}(g \rightarrow gg) \right]$$

Initial



$$\sigma^{H\bar{C}} = \int \left[\hat{\sigma}^{H\bar{C}}(gg \rightarrow J/\psi + gg) + \sum_{q=u,d,s} \hat{\sigma}^{H\bar{C}}(gg \rightarrow J/\psi + q\bar{q}) \right] dx_1 dx_2 G_g(x_1, \mu_f) G_g(x_2, \mu_f) \\ + \int \sum_{\alpha=u,d,s,\bar{u},\bar{d},\bar{s}} \hat{\sigma}^{H\bar{C}}(g\alpha \rightarrow J/\psi + g\alpha) [G_g(x_1, \mu_f) G_\alpha(x_2, \mu_f) + (x_1 \leftrightarrow x_2)] dx_1 dx_2$$

REAL



Hard Noncollinear



$$\sigma^R = \sigma_{add}^{HC} + \sigma^{H\bar{C}} + \int \left(\hat{\sigma}^S + \hat{\sigma}_f^{HC} + \hat{\sigma}_i^{HC} \right) G_g(x_1, \mu_f) G_g(x_2, \mu_f) dx_1 dx_2$$

Cross Section at NLO

$$\sigma^{NLO} = \sigma_{add}^{HC} + \sigma^{H\bar{C}} \\ + \int \left(\hat{\sigma}^B + \hat{\sigma}^V + \hat{\sigma}^S + \hat{\sigma}_f^{HC} + \hat{\sigma}_i^{HC} \right) G_g(x_1, \mu_f) G_g(x_2, \mu_f) dx_1 dx_2$$

$$2A_2^V + A_2^S = 0$$

$$2A_1^V + A_1^S + A_1^{g \rightarrow gg} + A_1^{g \rightarrow q\bar{q}} + 2A_1^{sc}(g \rightarrow gg) = 0$$



Finite

$dx_2 dt \rightarrow J dp_t dy$ is applied to obtain transverse momentum distribution

$$\begin{aligned}\sigma &= \int dx_1 dx_2 dt G_g(x_1, \mu_f) G_g(x_2, \mu_f) \frac{d\hat{\sigma}}{dt} \\ &= \int J dx_1 dp_t dy G_g(x_1, \mu_f) G_g(x_2, \mu_f) \frac{d\hat{\sigma}}{dt} \\ \frac{d\sigma}{dp_t} &= \int J dx_1 dy G_g(x_1, \mu_f) G_g(x_2, \mu_f) \frac{d\hat{\sigma}}{dt}\end{aligned}$$

polarization parameter α is defined as:

$$\alpha(p_t) = \frac{\frac{d\sigma_T}{dt} - 2 \frac{d\sigma_L}{dt}}{\frac{d\sigma_T}{dt} + 2 \frac{d\sigma_L}{dt}}$$

$\alpha = +1$: fully transverse polarization

$\alpha = -1$: fully longitudinal polarization

$$p_1 = x_1 \frac{\sqrt{S}}{2} (1, 0, 0, 1)$$

$$p_2 = x_2 \frac{\sqrt{S}}{2} (1, 0, 0, -1)$$

$$m_t = \sqrt{M_{J/\psi}^2 + p_t^2}$$

$$p_3 = (m_t \cosh y, p_t, 0, m_t \sinh y)$$

$$x_t = \frac{2m_t}{\sqrt{S}}$$

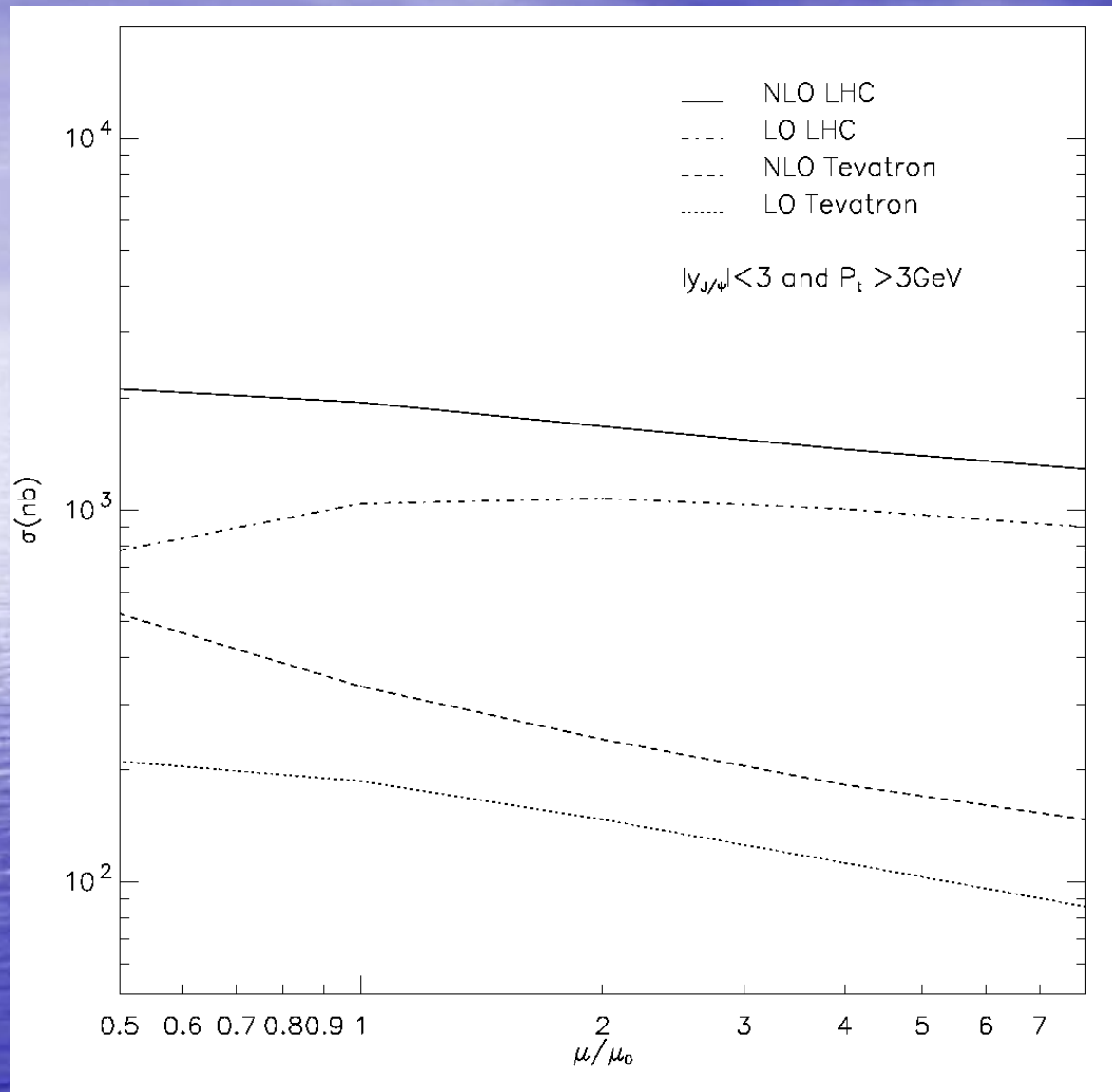
$$\tau = \frac{m_4^2 - M_{J/\psi}^2}{\sqrt{S}}$$

$$J = \frac{4x_1 x_2 p_t}{2x_1 - x_t e^y}$$

$$x_2 = \frac{2\tau + x_1 x_t e^{-y}}{2x_1 - x_t e^y}$$

$$x_1|_{min} = \frac{2\tau + x_t e^y}{2 - x_t e^{-y}}$$

$d\sigma_T/dt, d\sigma_L/dt$ are differential cross section of transverse polarization and longitudinal one respectively



$$\left| R_s^{J/\psi}(0) \right|^2 = 0.810 \text{ GeV}^3$$

$$m_c = 1.5 \text{ GeV}$$

$$\mu_r = \mu_f = \mu$$

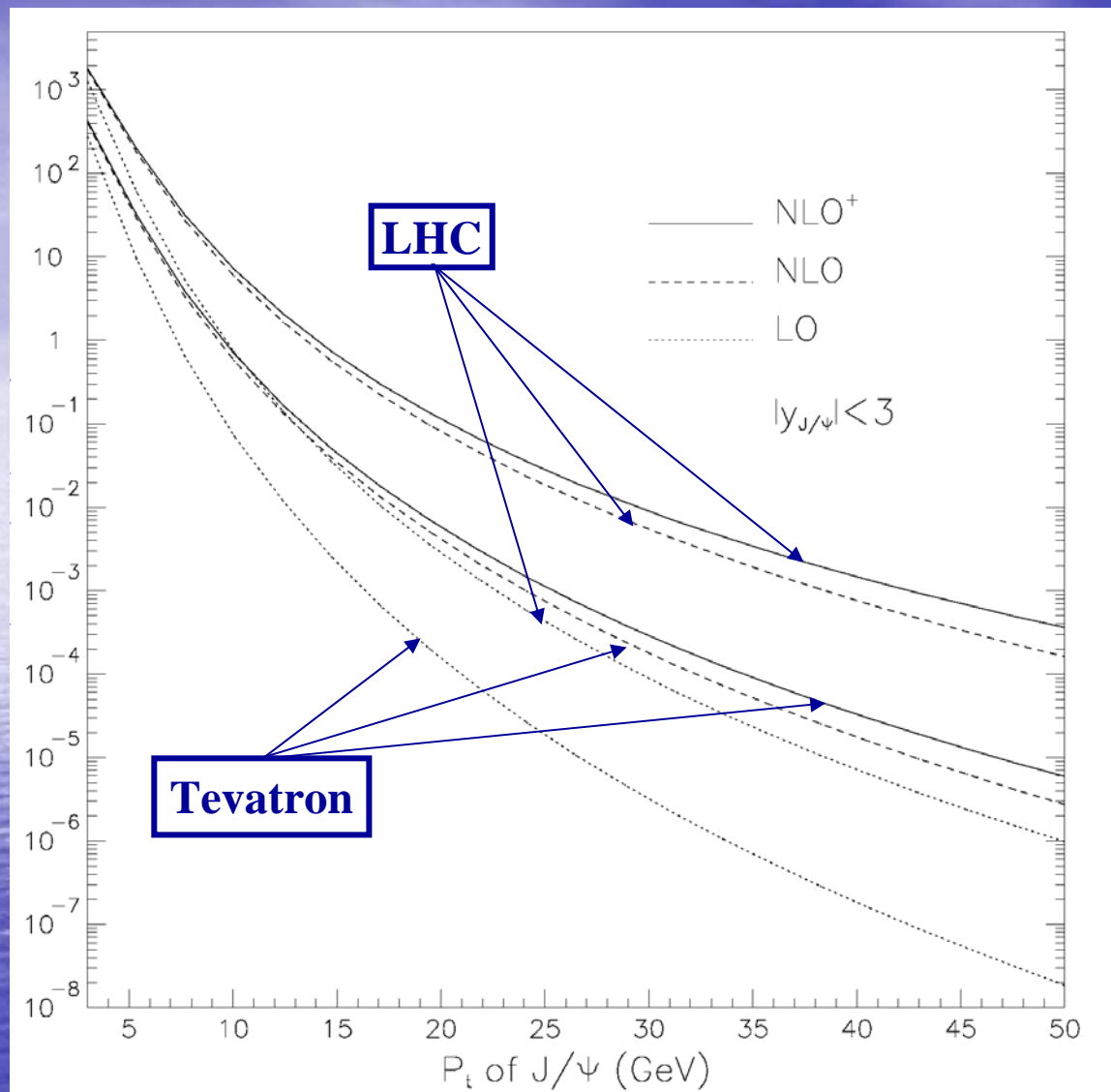
$$\mu_0 = \sqrt{(2m_c)^2 + p_t^2}$$

$$\sqrt{s}_{\text{Tevatron}} = 1.96 \text{ TeV}$$

$$\sqrt{s}_{\text{LHC}} = 14 \text{ TeV}$$

- The NLO QCD corrections boost the total cross section by a factor of about 2
- The scale dependence at NLO is not improved

Total cross section of J/ψ production as function of the renormalization scale μ_r and factorization scale μ_f



$$\mu_r = \mu_f = \sqrt{(2m_c)^2 + p_t^2}$$

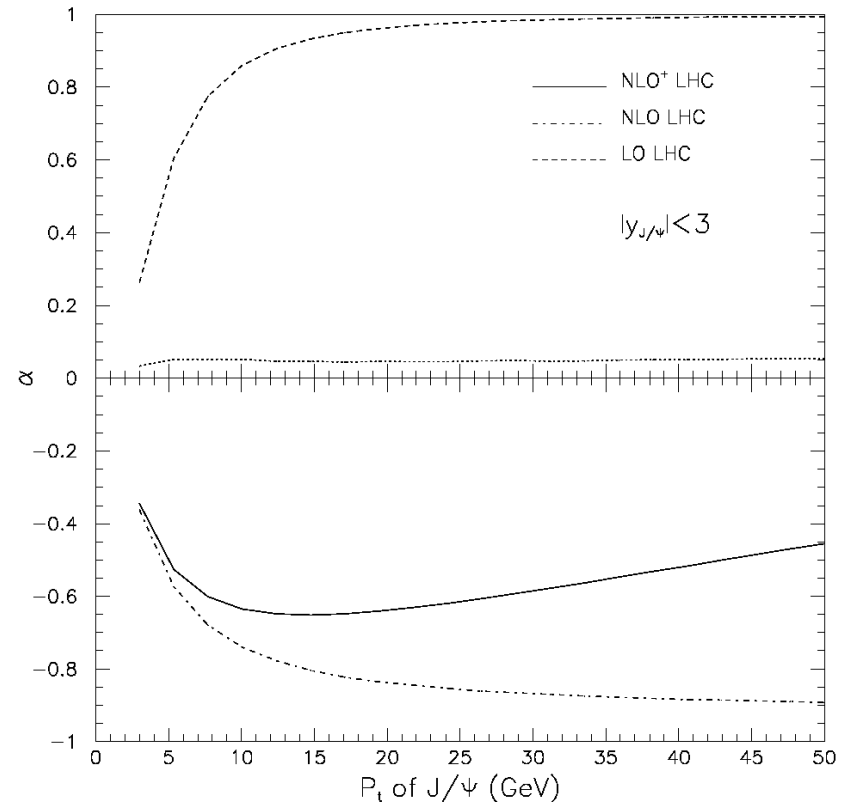
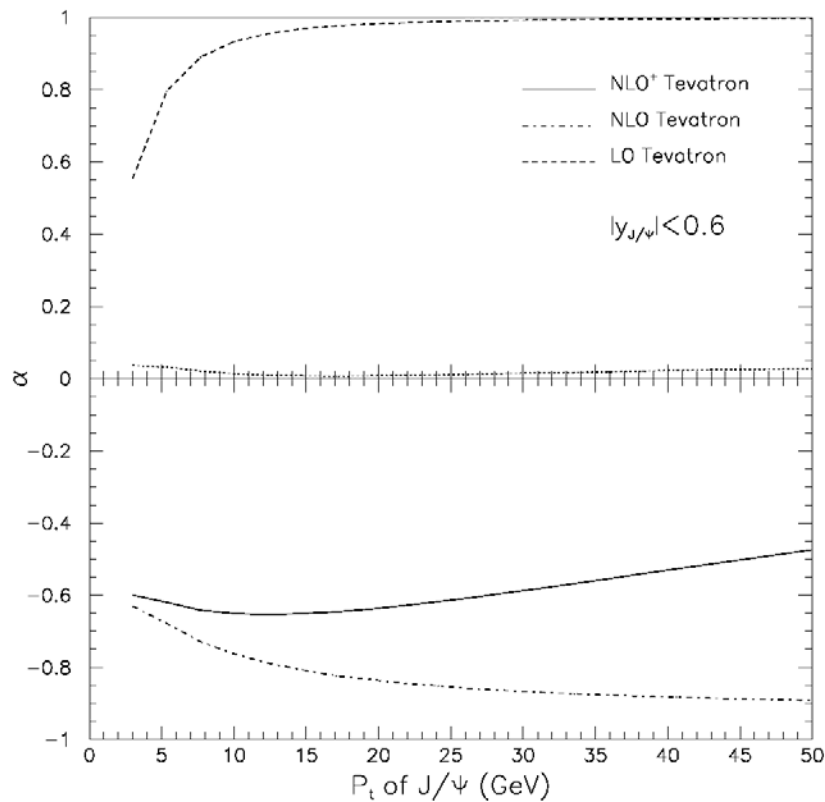
Upper: LHC
Lower: Tevatron

**contribution of NLO
correction becomes
larger as p_t increases**

2-3 order larger in
magnitude at $p_t=50$ GeV

Transverse momentum distribution of J/ψ production

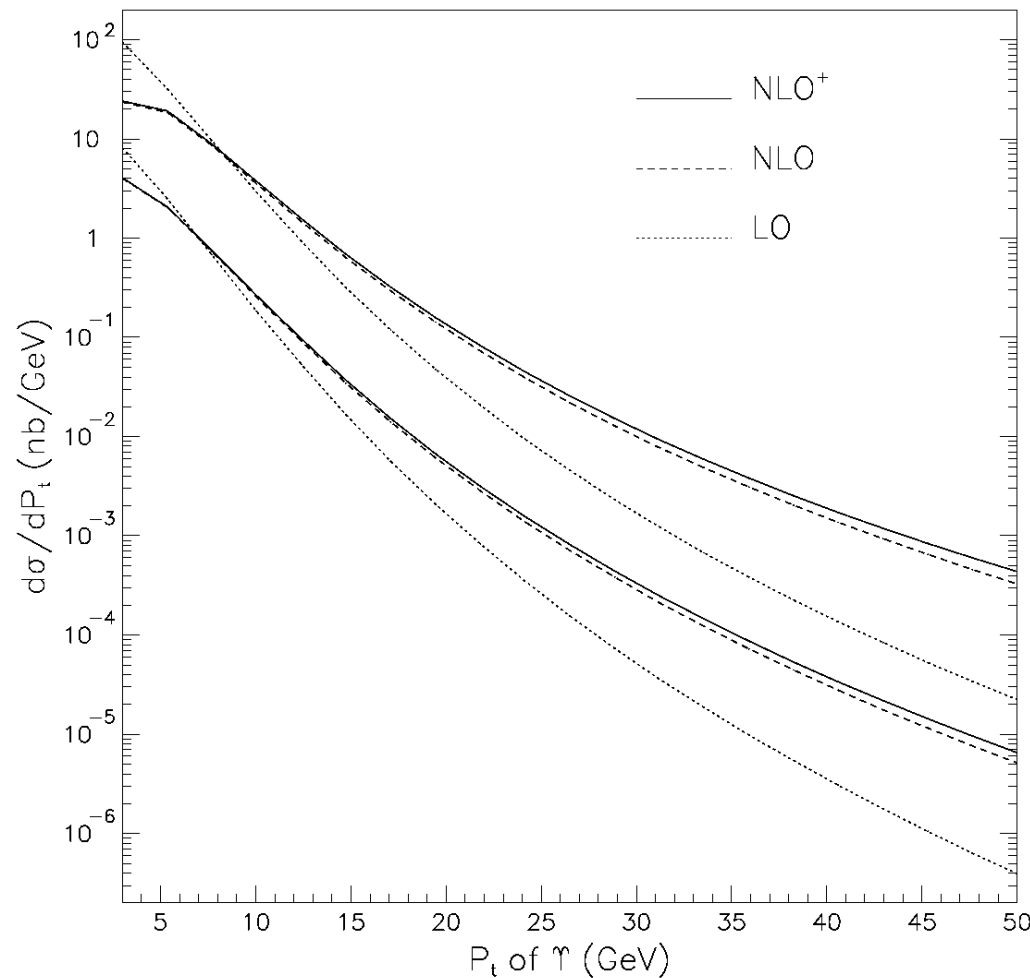
NLO⁺ : contribution from $J/\psi + c\bar{c}$ is included



Transverse momentum distribution of J/ψ polarization parameter α

J/ψ polarization status drastically changes from transverse polarization dominant at LO into longitudinal polarization dominant at NLO

This work is published in Phys. Rev. Lett. **100**, 232001 (2008),
arXiv:0802.3727.



$$m_c \leftrightarrow m_b$$

$$M_{J/\psi} \leftrightarrow M_{\Upsilon}$$

$$R_s(0)^{J/\psi} \leftrightarrow R_s(0)^{\Upsilon}$$

$$n_f = 3 \leftrightarrow n_f = 4$$

Upper: LHC

Lower: Tevatron

$$|R_s^Y(0)|^2 = 0.479 \text{ GeV}^3$$

$$m_b = 4.75 \text{ GeV}$$

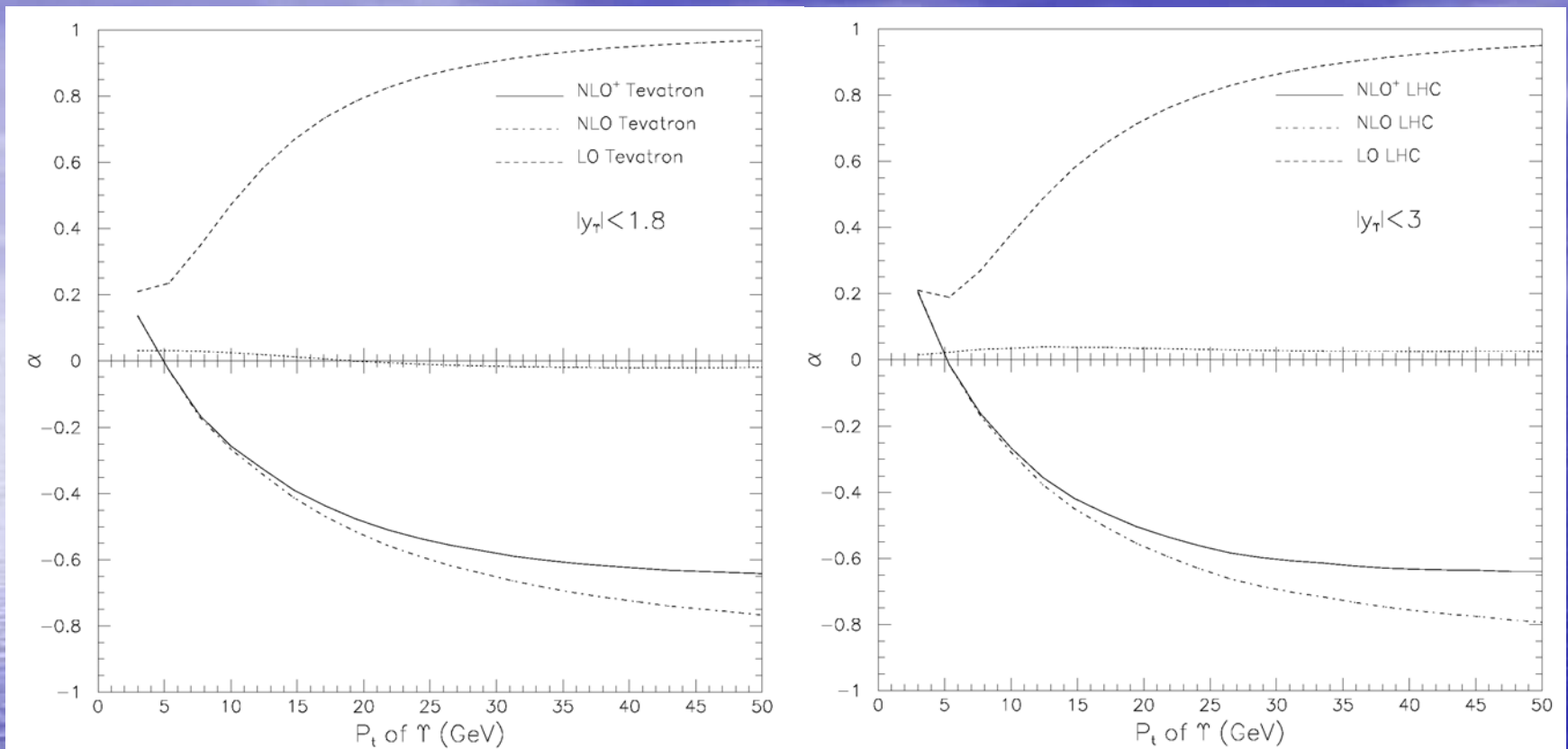
$$\mu_r = \mu_f = \sqrt{(2m_b)^2 + p_t^2}$$

$$|y_Y|_{\text{Tevatron}} < 1.8$$

$$|y_Y|_{\text{LHC}} < 3$$

Transverse momentum distribution of Υ production

NLO^+ : contribution from $Y + b\bar{b}$ is included



Transverse momentum distribution of the polarization parameter α

Polarization also changes greatly with NLO QCD corrections included

This work was presented in arXiv:0805.2469, is published in Physical Review D (long article with more details).

Summary for color singlet

- ❁ The J/ψ polarization is dramatically changed from transverse polarization dominant at LO into longitudinal polarization dominant at NLO. Even though our results are in a more longitudinal polarization state than the recent experimental result at Tevatron, it raises a hope to solve the large discrepancy between theoretical prediction and experimental measurement on J/ψ polarization.
- ❁ Next important step is to calculate the NLO corrections to J/ψ hadronproduction via color octet state.

NLO QCD corrections to J/ψ production via S-wave color octet states

3 tree processes at LO

At NLO

$$g(p_1) + g(p_2) \rightarrow J/\psi \left[{}^1S_0^{(8)}, {}^3S_1^{(8)} \right] (p_3) + g(p_4), \quad (267, 413)$$

$$g(p_1) + q(p_2) \rightarrow J/\psi \left[{}^1S_0^{(8)}, {}^3S_1^{(8)} \right] (p_3) + q(p_4), \quad (49, 111)$$

$$q(p_1) + \bar{q}(p_2) \rightarrow J/\psi \left[{}^1S_0^{(8)}, {}^3S_1^{(8)} \right] (p_3) + g(p_4). \quad (49, 111)$$

Real Correction (8 processes at NLO)

$$gg \rightarrow J/\psi \left[{}^1S_0^{(8)}, {}^3S_1^{(8)} \right] gg, \quad gg \rightarrow J/\psi \left[{}^1S_0^{(8)}, {}^3S_1^{(8)} \right] q\bar{q},$$

$$gq \rightarrow J/\psi \left[{}^1S_0^{(8)}, {}^3S_1^{(8)} \right] gq, \quad q\bar{q} \rightarrow J/\psi \left[{}^1S_0^{(8)}, {}^3S_1^{(8)} \right] gg,$$

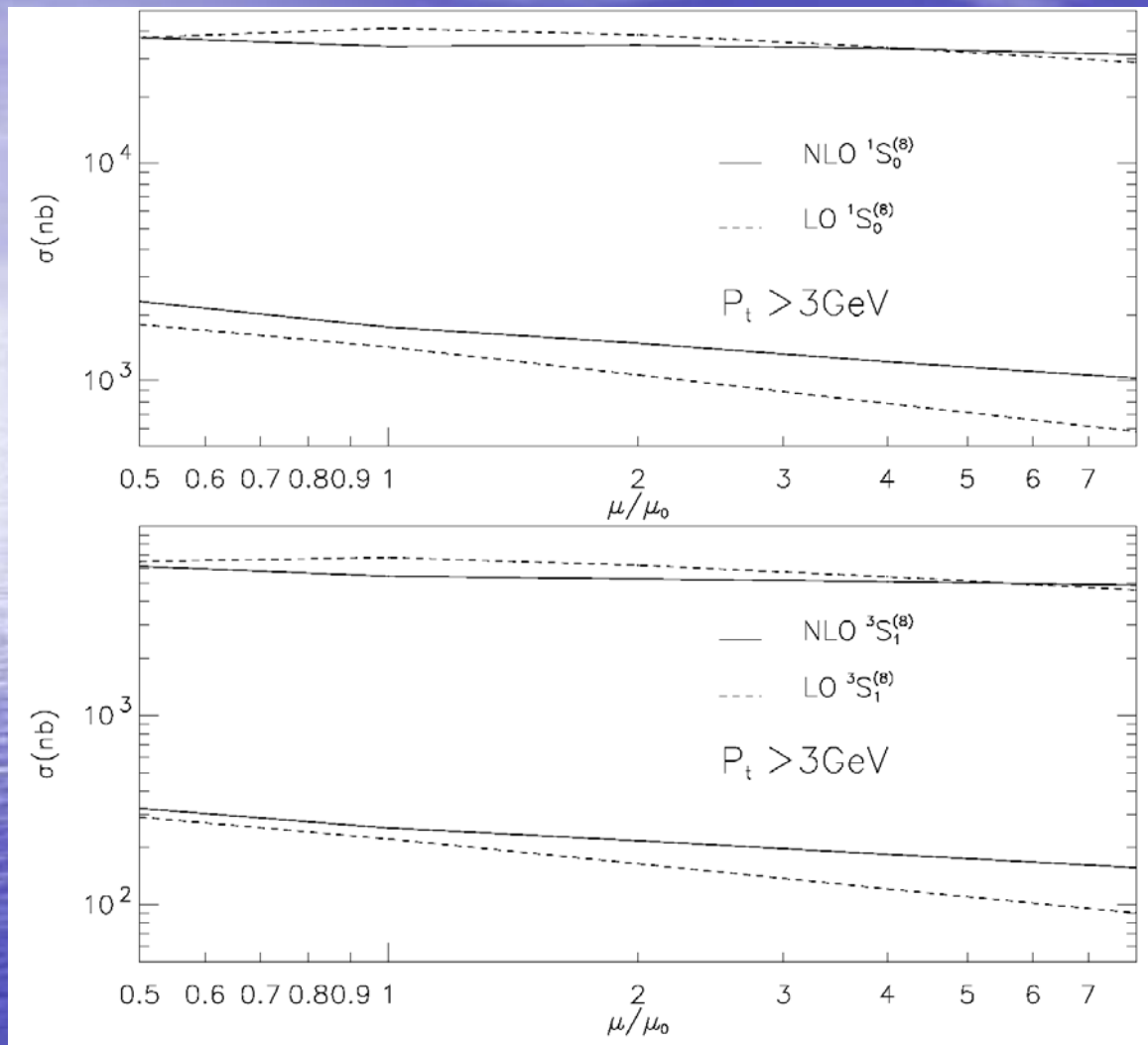
$$q\bar{q} \rightarrow J/\psi \left[{}^1S_0^{(8)}, {}^3S_1^{(8)} \right] q\bar{q}, \quad q\bar{q} \rightarrow J/\psi \left[{}^1S_0^{(8)}, {}^3S_1^{(8)} \right] q'\bar{q}',$$

$$qq \rightarrow J/\psi \left[{}^1S_0^{(8)}, {}^3S_1^{(8)} \right] qq, \quad qq' \rightarrow J/\psi \left[{}^1S_0^{(8)}, {}^3S_1^{(8)} \right] qq',$$

$$\begin{aligned}
\delta Z_m^{OS} &= -3C_F \frac{\alpha_s}{4\pi} \left[\frac{1}{\epsilon_{UV}} - \gamma_E + \ln \frac{4\pi\mu_r^2}{m_c^2} + \frac{4}{3} \right] \\
\delta Z_2^{OS} &= -C_F \frac{\alpha_s}{4\pi} \left[\frac{1}{\epsilon_{UV}} + \frac{2}{\epsilon_{IR}} - 3\gamma_E + 3 \ln \frac{4\pi\mu_r^2}{m_c^2} + 4 \right] \\
\delta Z_{2l}^{OS} &= -C_F \frac{\alpha_s}{4\pi} \left[\frac{1}{\epsilon_{UV}} - \frac{1}{\epsilon_{IR}} \right] \\
\delta Z_3^{OS} &= \frac{\alpha_s}{4\pi} \left[(\beta_0 - 2C_A) \left(\frac{1}{\epsilon_{UV}} - \frac{1}{\epsilon_{IR}} \right) \right] \\
\delta Z_g^{\overline{\text{MS}}} &= -\frac{\beta_0}{2} \frac{\alpha_s}{4\pi} \left[\frac{1}{\epsilon_{UV}} - \gamma_E + \ln(4\pi) \right]
\end{aligned}$$

The renormalization constant of light quark field is also needed in color-octet case.

The renormalization constants



Total cross section of J/ψ production as function of the renormalization and factorization scale via S-wave color octet states

Upper curves: LHC
Lower curves: Tevatron

$$\mu_r = \mu_f = \mu$$

$$\mu_0 = \sqrt{(2m_c)^2 + p_t^2}$$

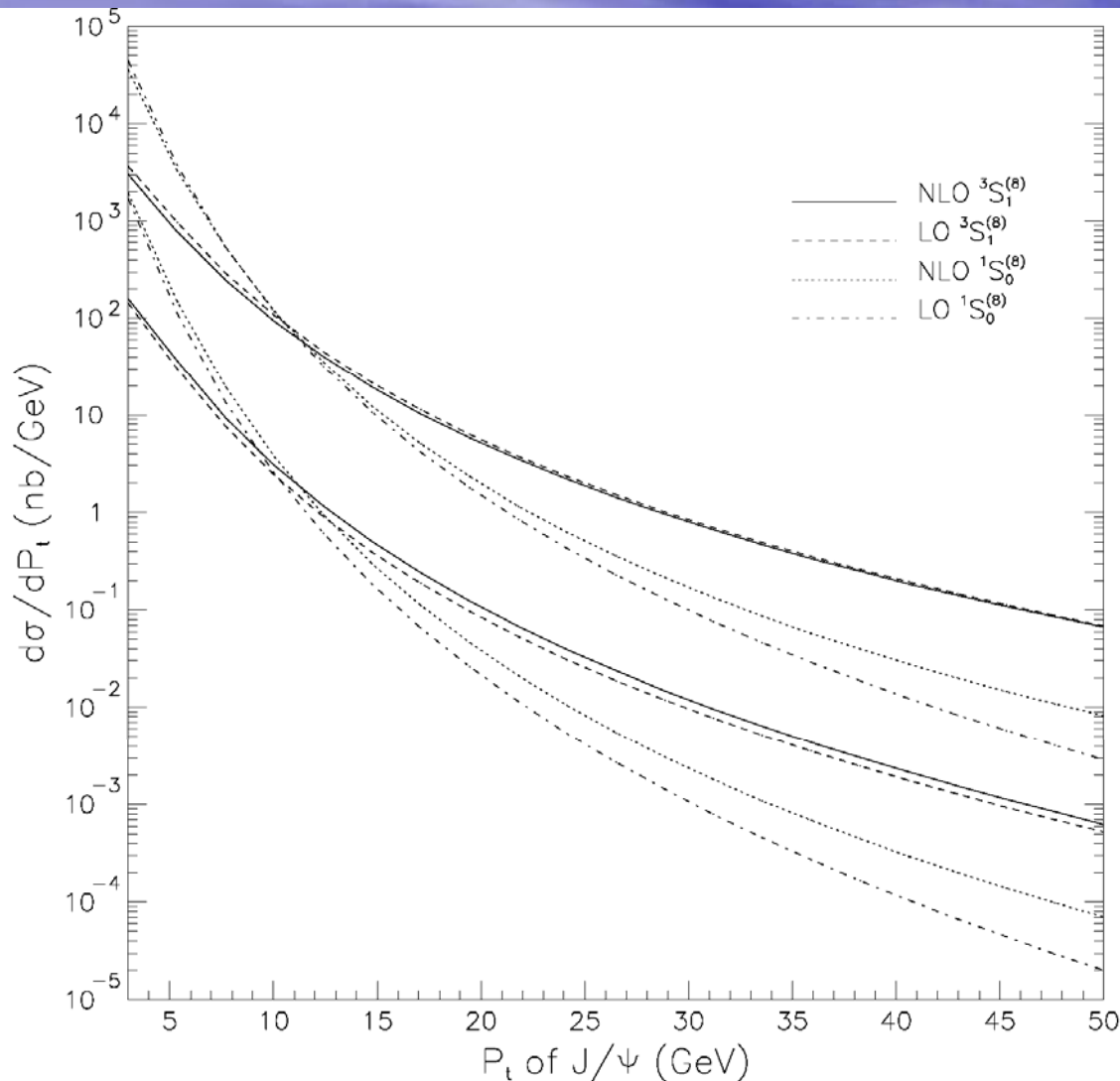
$$|y_{J/\psi}|_{\text{Tevatron}} < 0.6$$

$$|y_{J/\psi}|_{\text{LHC}} < 3$$

K factors at $\mu = \mu_0$:

	Tevatron	LHC
$1S_0^{(8)}$	1.235	0.826
$3S_1^{(8)}$	1.119	0.800

The NLO QCD corrections don't change the total cross section very much.



$$\mu_r = \mu_f = \sqrt{(2m_c)^2 + p_t^2}$$

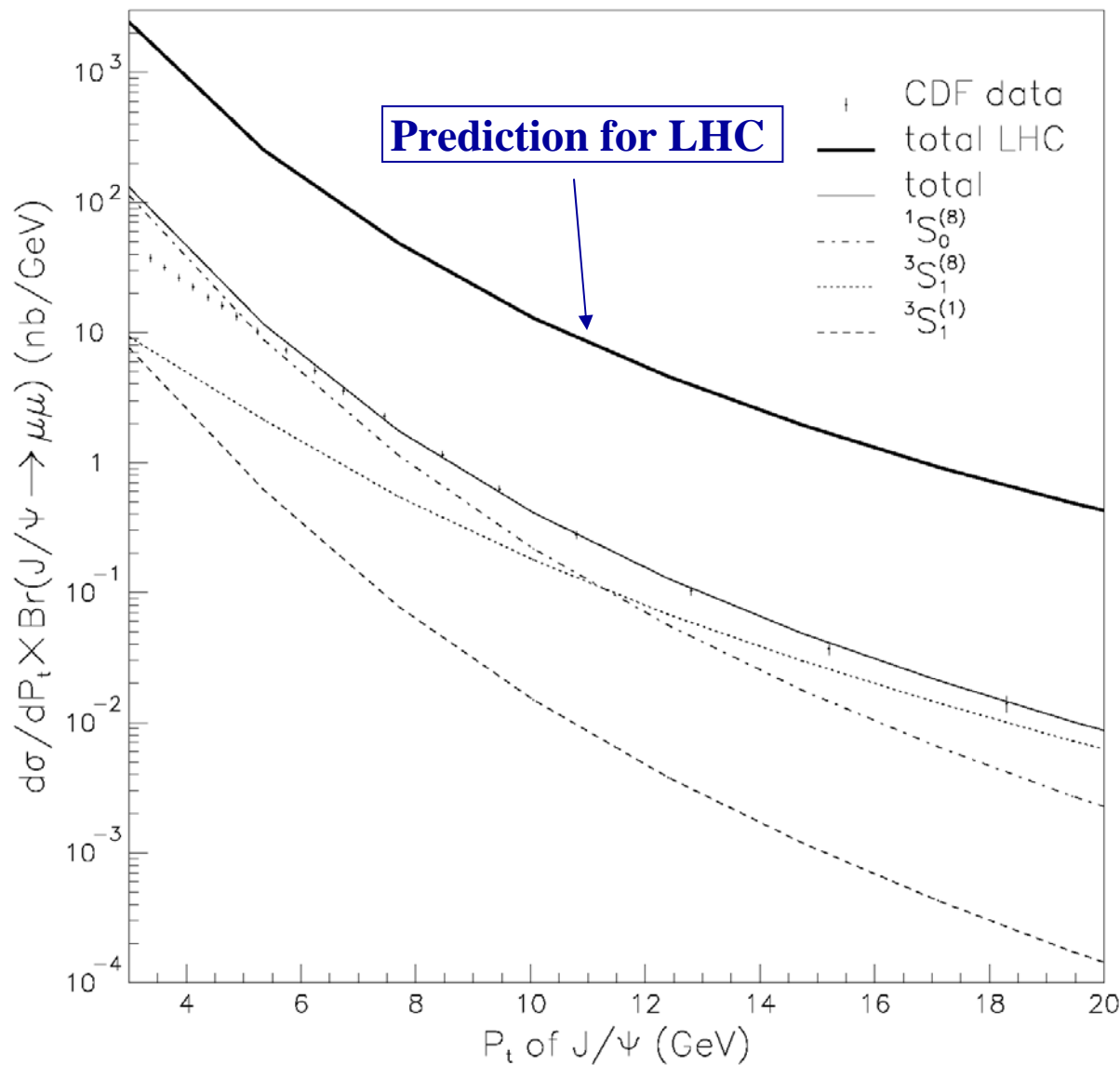
$$|y_{J/\psi}|_{\text{Tevatron}} < 0.6$$

$$|y_{J/\psi}|_{\text{LHC}} < 3$$

Upper: LHC
Lower: Tevatron

**Only slight change appears
when the NLO QCD
corrections are included.**

Transverse momentum distribution of J/ψ production
via S-wave color octet states



$$\mu_r = \mu_f = \sqrt{(2m_c)^2 + p_t^2}$$

$$|y_{J/\psi}|_{\text{Tevatron}} < 0.6$$

$$|y_{J/\psi}|_{\text{LHC}} < 3$$

Our fitted matrix elements:

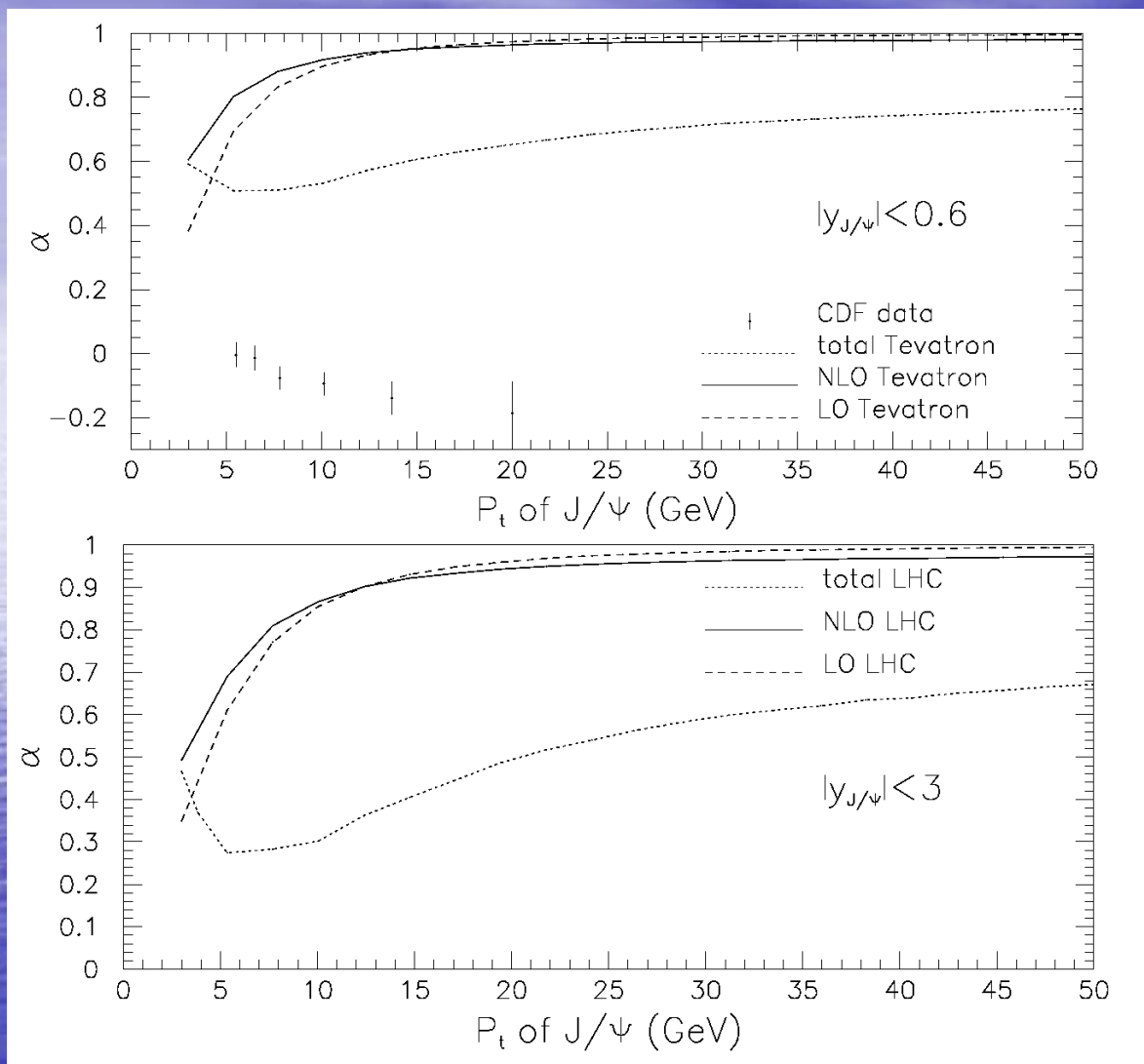
$$\langle \mathcal{O}_8^\psi(3S_1) \rangle = 0.0045 \text{ GeV}^3$$

$$\langle \mathcal{O}_8^\psi(1S_0) \rangle = 0.0760 \text{ GeV}^3$$

Notes in fitting

- Experimental data with $p_t < 6 \text{ GeV}$ has been abandoned
- Feed down from ψ' has been included by multiplying a factor of $B(\psi' \rightarrow J/\psi + X) \times \langle \mathcal{O}_n^{\psi'} \rangle / \langle \mathcal{O}_n^\psi \rangle$
- Contribution via P-wave has not been included

Transverse momentum distribution of **prompt** J/ψ production



Upper: Tevatron
Lower: LHC


- ❁ Dash and solid lines are LO and NLO results for J/psi polarization via color octet state 3S_1 . It has changed little when NLO QCD corrections are included.
- ❁ 1S_0 gives contribution to $\alpha=0$.
- ❁ Obvious gap is shown between our prediction and experimental data at Tevatron.

This work was presented in
arXiv:0805.4751,.

Transverse momentum distribution of polarization
parameter α for prompt J/ ψ

Conclusion and Summary

- ❁ Comparing the theoretical results calculated up to NLO with the experimental measurements at Tevatron, obvious gap is shown, even though both color singlet and octet are included.
- ❁ NLO corrections to J/ψ production via P-wave color octet state 3P_J and J/ψ production by feed-down from χ_{cJ} haven't been calculated yet.
- ❁ If we assume that the NLO QCD corrections to the two P-wave states are just as those for the S-wave color octet states, it is reasonable for us to reach the conclusion that the large discrepancy of J/ψ polarization between theoretical prediction and the experimental measurement cannot be solved by just including NLO corrections within NRQCD framework and new solutions should be considered.



$$e^+e^- \rightarrow J/\psi + gg$$

LO NRQCD Prediction:

$$e^+e^- \rightarrow J/\psi + c\bar{c} \quad 0.07 - 0.20 \text{ pb}$$

$$e^+e^- \rightarrow J/\psi + gg \quad 0.15 - 0.3 \text{ pb}$$

$$e^+e^- \rightarrow J/\psi^{(8)}(^3P_J, ^1S_0) + g \quad 0.3 - 0.8 \text{ pb}$$

Experimental Data:

$$BABAR : 2.54 \pm 0.21 \pm 0.21 \text{ pb}$$

$$Belle : 1.45 \pm 0.10 \pm 0.13 \text{ pb} \quad e^+e^- \rightarrow J/\psi + X$$

$$CLEO : 1.9 \pm 0.20 \text{ pb}$$

$$Belle : 0.87_{-0.19}^{+0.21} \pm 0.17 \text{ pb} \quad e^+e^- \rightarrow J/\psi + c\bar{c} + X$$

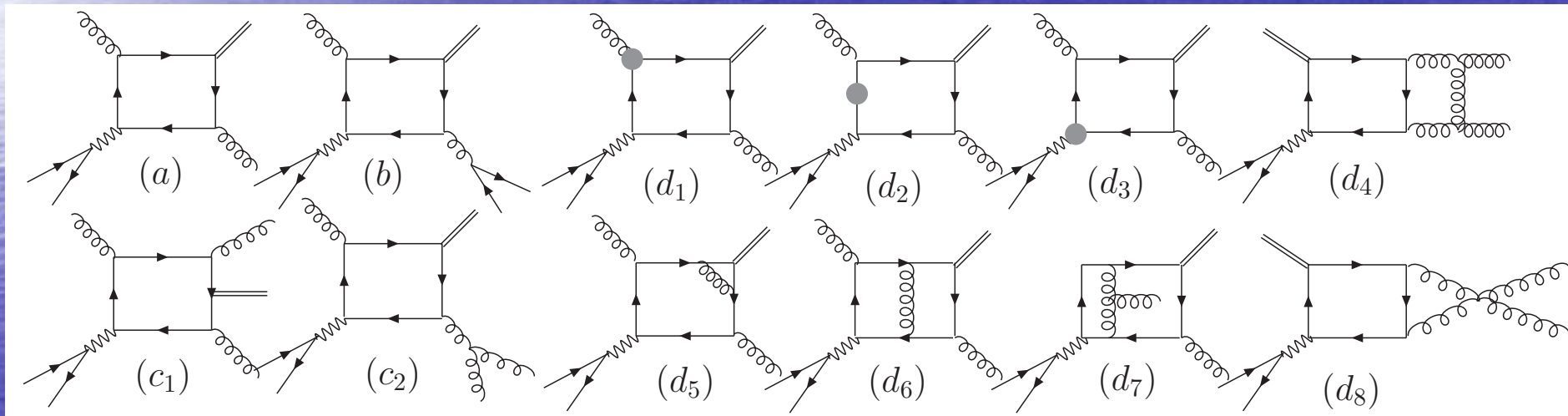
➡ $\sigma[e^+e^- \rightarrow J/\psi + X(\text{non } c\bar{c})] \simeq 0.6 \text{ pb}$

2. Calculation and results for $e^+e^- \rightarrow J/\Psi gg$ at NLO

$e^+e^- \rightarrow J/\Psi + gg$ LO (a) , 6; NLO (d1—d8), 111

$e^+e^- \rightarrow J/\Psi + ggg$ Real (c1,c2), 36

$e^+e^- \rightarrow J/\Psi + gqq$ Real (b), 6



Dimensional regularization has been adopted for isolating the ultraviolet (UV) and infrared (IR) singularities. Coulomb Singularity is isolated by v and mapped into the cc wave function.

$$\sigma^{(0)} = -\frac{\alpha^2 \alpha_s^2 e_c^2 |R_s(0)|^2}{9m_c^5 \hat{s}^3 (\hat{s} - 1)} 18(\hat{s}^2 - 2\hat{s} + 2) +$$

$$\frac{2\hat{s}(5\hat{s}^2 - 14\hat{s} + 3)}{\hat{s} - 1} \ln(\hat{s}) + \frac{2(4\hat{s}^2 - 9\hat{s} + 8)\beta}{\hat{s} - 1} \ln(2\hat{s} - 1 - 2\beta)$$

$$+ \frac{2\hat{s}^2 - \hat{s}^2 - 12\hat{s} + 8}{\hat{s} - 1} \left[\text{Li}_2\left(\frac{2(\hat{s} - 1)}{\hat{s} + \beta - 1}\right) + \text{Li}_2\left(\frac{2(\hat{s} - 1)}{\hat{s} - \beta - 1}\right) \right]$$

Where $\hat{s} = s/(2m_c)^2$ $\beta = \sqrt{\hat{s}(\hat{s} - 1)}$. $R_s(0)$ is extracted from the
 Leptonic decay width at
 Renormalization Scheme: NLO formulation.

$$\delta Z_m^{OS} = -3C_F \frac{\alpha_s}{4\pi} \left[\frac{1}{\epsilon_{UV}} - \gamma_E + \ln \frac{4\pi \mu_r^2}{m_c^2} + \frac{4}{3} \right],$$

$$\delta Z_2^{OS} = -C_F \frac{\alpha_s}{4\pi} \left[\frac{1}{\epsilon_{UV}} + \frac{2}{\epsilon_{IR}} - 3\gamma_E + 3 \ln \frac{4\pi \mu_r^2}{m_c^2} + 4 \right],$$

$$\delta Z_{2l}^{OS} = -C_F \frac{\alpha_s}{4\pi} \left[\frac{1}{\epsilon_{UV}} - \frac{1}{\epsilon_{IR}} \right],$$

$$\delta Z_3^{OS} = \frac{\alpha_s}{4\pi} \left[(\beta_0 - 2C_A) \left(\frac{1}{\epsilon_{UV}} - \frac{1}{\epsilon_{IR}} \right) \right],$$

$$\delta Z_g^{\overline{\text{MS}}} = -\frac{\beta_0}{2} \frac{\alpha_s}{4\pi} \left[\frac{1}{\epsilon_{UV}} - \gamma_E + \ln(4\pi) \right],$$

The two-cutoff phase space slicing method is adopted by introducing two small cutoffs δ_s, δ_c .

$$\sigma^R = \sigma^S + \sigma^{HC} + \sigma^{H\bar{C}}$$

For Soft region:

$$d\sigma^S = d\sigma^{(0)} \frac{\alpha_s}{2\pi} \frac{\Gamma(1-\epsilon)}{\Gamma(1-2\epsilon)} \left(\frac{4\pi\mu^2}{s} \right)^\epsilon \left(\frac{A_2^S}{\epsilon^2} + \frac{A_1^S}{\epsilon} + A_0^S \right),$$

$$A_2^S = 6, \quad A_1^S = -12 \ln \delta_s - 6 \ln(\sin^2 \frac{\theta_g}{2}),$$

$$A_0^S = \frac{(A_1^S)^2}{12} + 6 \text{Li}_2(\cos^2 \frac{\theta_g}{2}),$$

For Hard Collinear region:

$$d\sigma^{HC} = d\sigma^{(0)} \frac{\alpha_s}{2\pi} \frac{\Gamma(1-\epsilon)}{\Gamma(1-2\epsilon)} \left(\frac{4\pi\mu^2}{s} \right)^\epsilon \left(\frac{A_1^{HC}}{\epsilon} + A_0^{HC} \right),$$

$$A_1^{HC} = 11 + 6 \ln \delta_s^{(4)} + 6 \ln \delta_s^{(5)} - \frac{2}{3} n_{lf},$$

$$A_0^{HC} = \frac{67}{3} - \frac{10}{9} n_{lf} - 2\pi^2 - 3 \ln^2 \delta_s^{(4)} - 3 \ln^2 \delta_s^{(5)} - \ln \delta_c A_1^{HC},$$

Where $\delta_s^{(j)} = \delta_s / [1 - (p_3 + p_j)^2/s]$

The total cross section at NLO for $e^+e^- \rightarrow J/\psi + gg$:

$$\sigma^{(1)} = \sigma^{(0)} \left\{ 1 + \frac{\alpha_s(\mu)}{\pi} \left[a(\hat{s}) + \beta_0 \ln\left(\frac{\mu}{2m_c} \right) \right] \right\}$$

m_c (GeV)	$\alpha_s(2m_c)$	$\sigma^{(0)}$ (pb)	$\sigma^{(1)}$ (pb)	$K = \sigma^{(1)} / \sigma^{(0)}$	$a(\hat{s})$
1.4	0.267	0.341	0.409	1.20	2.35
1.5	0.259	0.308	0.373	1.21	2.57
1.6	0.252	0.279	0.344	1.23	2.89

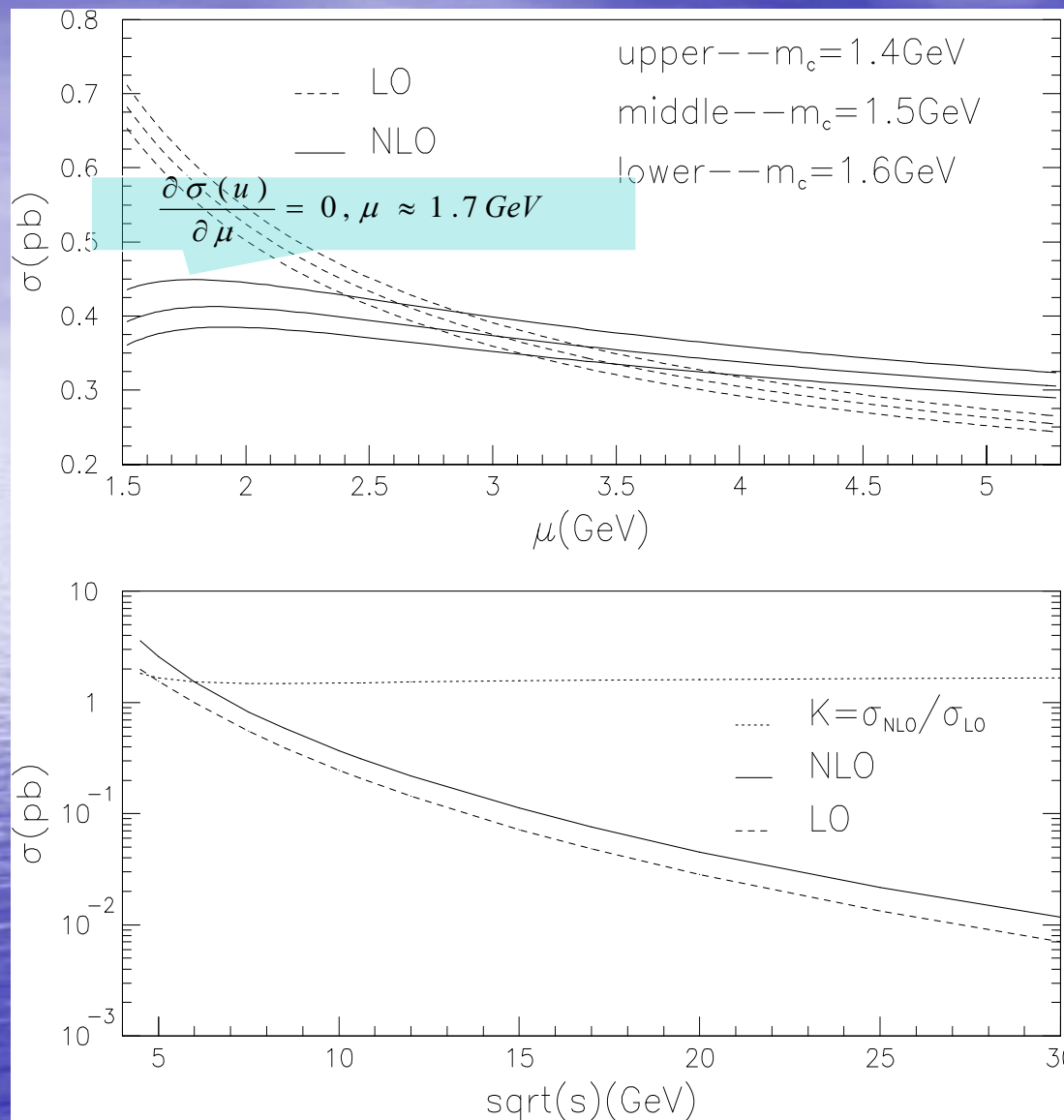
$$|R_s(0)|^2 = 0.944 \text{ GeV}^3, m_c = 1.5 \text{ GeV}, \mu = 2m_c, \hat{s} = s/(2m_c)^2$$

$$1.7(R_0^{NLO} / R_0^{LO}) \times 1.2(K - \text{factor})$$

Ψ' Feed-down

Indicate by the experiment

$$(0.294 - -0.45 \text{ pb}) \times 1.27 \approx 0.373 - 0.57 \text{ pb} \rightarrow 0.6 \text{ pb}$$



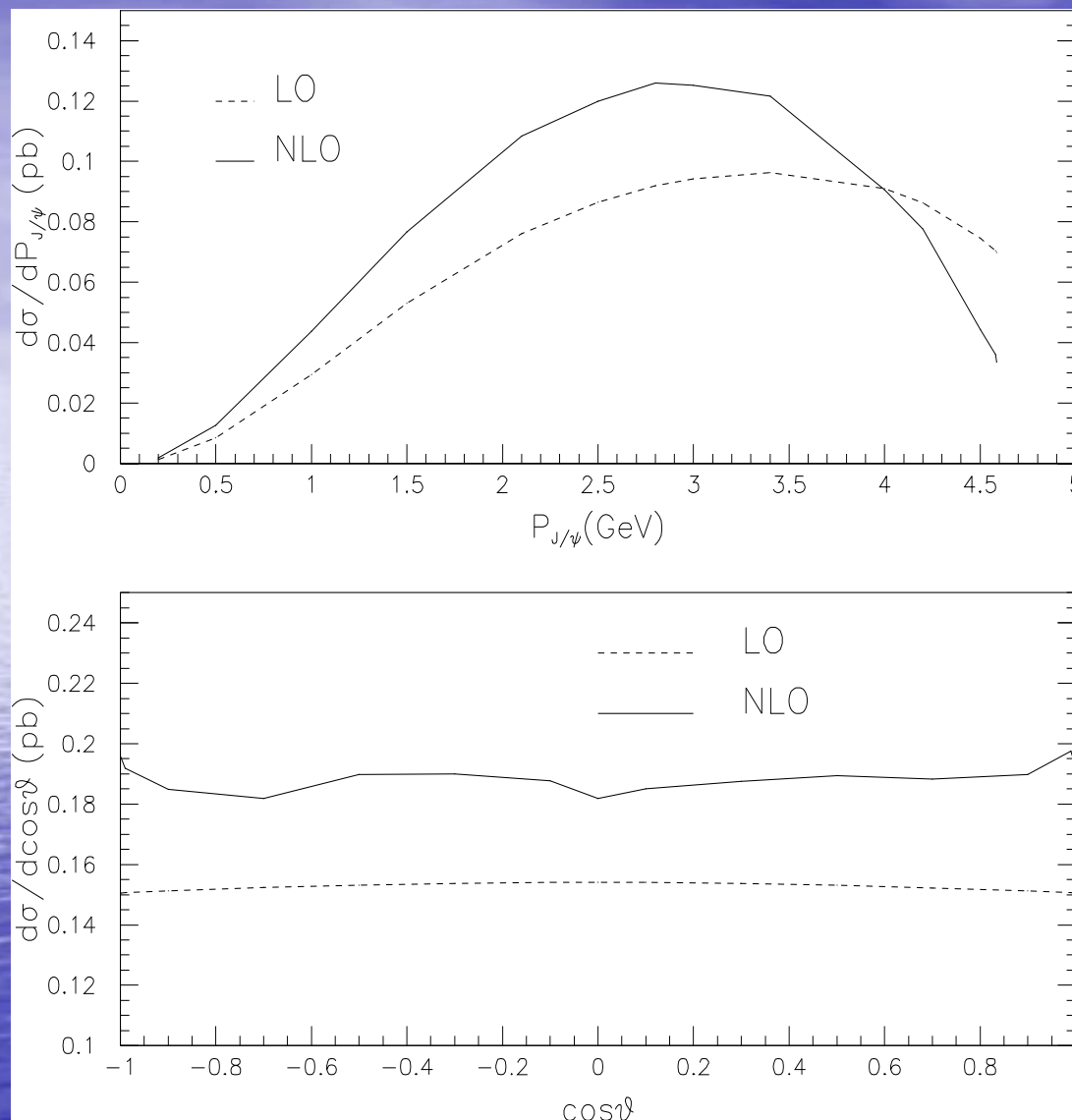
The scale dependence of cross section has been improved at NLO.

$$\sqrt{s} = 10.6 \text{ GeV}$$

The K factor does not change very much as center-of-mass energy increases.

$$\mu = \sqrt{s}/2$$

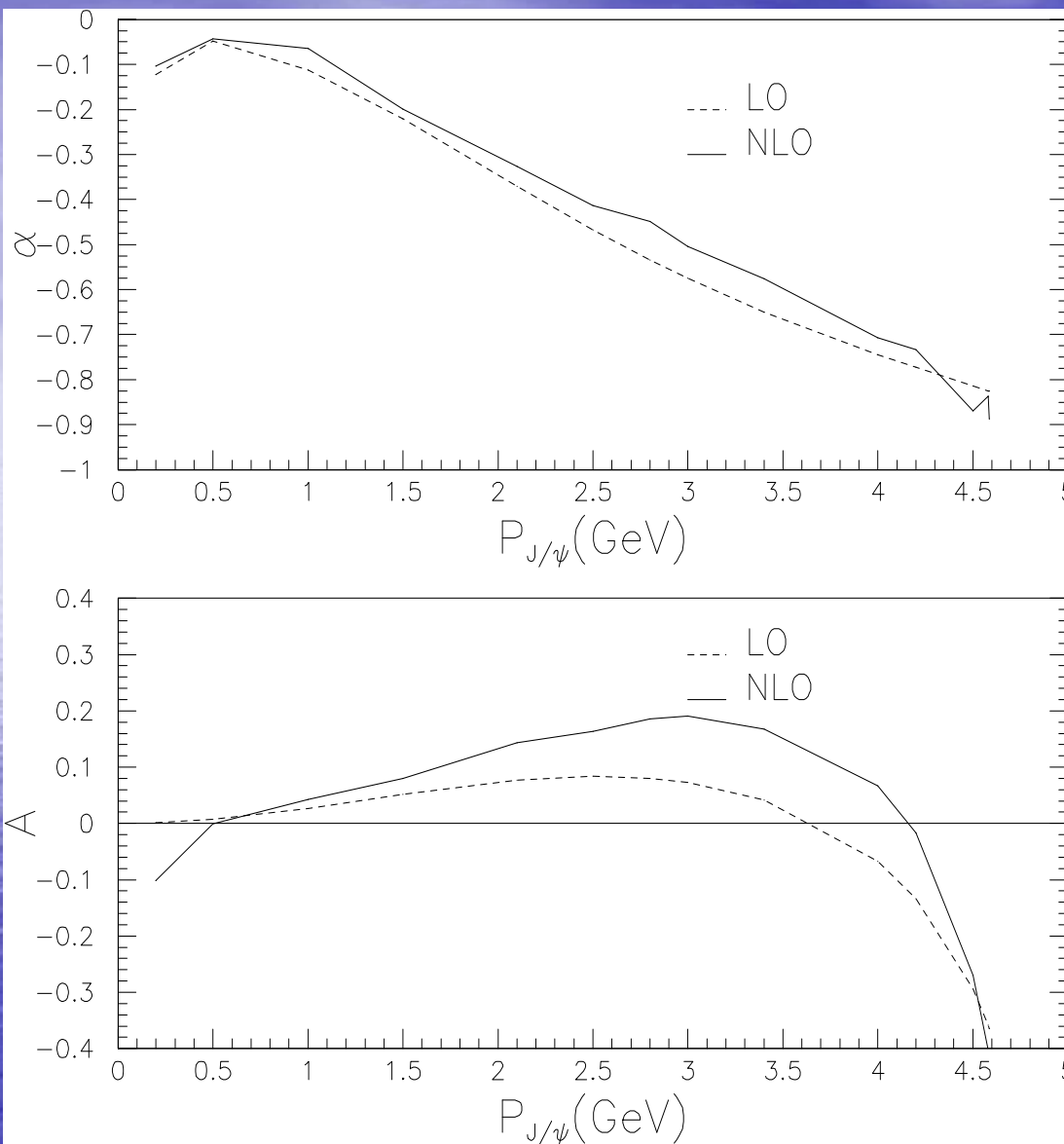
Cross section as function of the renormalization scale and center-of-mass energy.



The differential cross section decreases faster near right bound.

The angular distribution changes slightly except a factor of about 1.2.

Differential cross section as function of the momentum of J/ψ and the angle between J/ψ and the beam.



Both the polarization factor and the angular distribution coefficient do not change very much at NLO.

$$\alpha = \frac{\sigma_T - 2\sigma_L}{\sigma_T + 2\sigma_L}$$

$$\frac{d\sigma}{dP_{J/\psi} d\cos\theta}$$

$$= S(P_{J/\psi})[1 + A(P_{J/\psi})\cos^2\theta]$$

Polarization and angular distribution parameters as
function of the momentum of J/ψ

Summary and Conclusion

- The J/ψ polarization is dramatically changed from transverse polarization dominant at LO into longitudinal polarization dominant at NLO.
- Comparing the theoretical results calculated up to NLO with the experimental measurements at Tevatron, obvious gap is shown, even though both color singlet and octet are included.
- the large discrepancy of J/ψ polarization between theoretical prediction and the experimental measurement cannot be solved by just including NLO corrections within NRQCD framework and new solutions should be considered.
- The convergence for the NLO QCD correction to $e^+e^- \rightarrow J/\Psi + gg$ is very good, and to compare the polarization and momentum distribution with experimental results should be a good test for QCD predictions

Introduction to FDC Loop

The background of the slide is a photograph of a vast, deep blue ocean stretching to the horizon. The sky above is a lighter blue with wispy white clouds. The sun is visible on the left side, creating a bright, shimmering reflection on the water's surface.

Brief Introduction to FDC package

Feynman Diagram Calculation(FDC).

This first version of FDC was presented at AIHENP93 workshop,1993.

FDC Homepage::

http://www.ihep.ac.cn/lunwen/wjx/public_html/index.html

FDC-LOOP

FDC-PWA

FDC-EMT

FDC-SM-and-Many-Extensions

FDC-NRQCD

FDC-MSSM

**Written in REDUCE,
RLISP,C++.
To generate Fortran**

Event Generator



Thanks !

What can we do with LHC?

Examine the color-octet mechanism:

The NRQCD matrix elements are determined by fitting the data at Tevatron. Will the data at LHC support it, or not? It's interesting to know.

More suitable for comparing with theory:

There will be more events at LHC than that at Tevatron in the regions with large transverse momentum where perturbative QCD are more effective.

Meanwhile, there also will be more events on Y production at LHC, which has larger scale than J/ψ production .